https://doi.org/10.5194/egusphere-2025-278
Preprint. Discussion started: 5 March 2025

Contrail models lacking post-fallstreak behavior could underpredict lifetime optical depth

Caleb Akhtar Martínez[1], Sebastian D. Eastham[2], Jerome P. Jarrett[1]

[1]Department of Engineering, University of Cambridge, Cambridge, CB2 1PZ, United Kingdom
[2]Department of Aeronautics, Imperial College London, London, SW7 2AZ, United Kingdom

Correspondence to: Caleb Akhtar Martínez (ca525@cam.ac.uk)

Abstract. Proposed optimized contrail avoidance schemes rely on being able to robustly predict which contrails cause the most climate warming. However, it has not yet been shown that different contrail models agree sufficiently to support the targeting of individual contrails by climate impact. To address this, we compare the most widespread contrail model, CoCiP, to a higher-fidelity contrail model, APCEMM, under parametrized meteorological conditions. The results show that the lifetime optical depth (a proxy for climate impact) in APCEMM is 3.8 times that in CoCiP, and that the models have opposite sensitivities of their lifetime optical depth to relative humidity. We argue that these differences are due to the differing representations of the distribution of ice particles in space and in size across the contrails. The use of a monodisperse ice particle size distribution in a Gaussian plume means that CoCiP models the contrail exclusively as an accelerating, falling mass - a fallstreak. The use of a spatially gridded and size-resolved aerosol scheme allows APCEMM to represent the separation of the precipitation plume from the contrail core, hence modelling behavior past the initial fallstreak phase. This behavior is consistent with prior large eddy simulation studies, and it accounts for 92 % of the aggregate APCEMM lifetime optical depth. This suggests that fallstreak-only simulation may underestimate contrail climate impact. While a strategy avoiding all contrail formation is still expected to yield a reduction in climate impact, implementing optimized strategies requires more research to establish confidence in model predictions.

1 Introduction

It is estimated that aviation generates 3.5 % of all anthropogenic effective radiative forcing (ERF) and that contrail cirrus contributes 67% more ERF than the carbon dioxide produced by aircraft (Lee et al., 2021). These estimates indicate that strategies aiming to reduce contrail cirrus could provide benefits of a similar magnitude as the elimination of aviation-induced CO_2 emissions. The simplest proposed strategy involves attempting to avoid all contrails, but optimized schemes targeting only the most warming contrails (Teoh et al. 2020a; Teoh et al. 2020b) are also under consideration to maximize the reduction in contrail warming while minimizing the number of required flight deviations.

Avoiding any contrail requires accurate prediction of contrail formation, but strategies involving optimized avoidance rely on contrail models to accurately predict net contrail warming in hypothetical scenarios. At present, the model most widely used for this purpose is CoCiP (Schumann, 2012). CoCiP simulates the contrail cross section as a descending Gaussian plume. It is computationally efficient, open-source, and has been used in ~50% of all relevant academic works (see Appendix F). However, noting the difficulty of directly observing aged contrails, CoCiP has mostly been calibrated against observations of young contrails (Schumann et al., 2017). There are also few evaluations of its performance against models

https://doi.org/10.5194/egusphere-2025-278
Preprint. Discussion started: 5 March 2025

with more complex contrail representations, such as APCEMM (Fritz et al., 2020). The lack of model intercomparison in the literature has been previously raised as a potential cause for concern (Teoh et al., 2024).

Since models have different criteria to determine contrail lifetime, understanding how long a contrail will survive for under different meteorological conditions is non-trivial. Consider long-lived contrails, which produce lower local radiative forcing (RF) over larger areas. Since the local RF of an ice cloud increases fastest with ice water content for thin contrails (Wolf et al., 2023) such large, thin contrails are expected to have greater total climate impact than narrower, more visible contrails. Disagreement over contrail lifetime could therefore imply disproportionate disagreement in total climate impact. Contrail lifetime is often underestimated because thin contrails are harder to detect from satellites. For a typical contrail simulated in APCEMM (Fig. 1), assuming an optical depth observability threshold of 0.1 (Kärcher et al., 2009), 25 % of the lifetime optical depth is produced in the unobservable period. Meanwhile, long-lived contrails are challenging to simulate in gridded models since they have cross sectional areas of ~100 km^2. With the high potential for climate impact and the difficulty of direct observation, model intercomparison of the predicted lifetime and lifetime optical depth can indicate which conditions produce consistent outcomes and which need additional research.

The limited comparisons that have already been performed for large eddy simulations indicate disagreement in this regard (Unterstrasser and Gierens, 2010a; Unterstrasser and Gierens, 2010b; Lewellen et al., 2014; Lewellen, 2014). Furthermore, existing comparisons between APCEMM and CoCiP (Akhtar Martinez and Jarrett, 2024; Xu, 2024) have shown some inconsistencies between the models, but no study to date has established the extent of the agreement between CoCiP and any higher-fidelity contrail model when considering the effect of variation in meteorological parameters or the degree of consistency in identifying which contrails will have the greatest climate impact.

This study addresses this gap through a structured comparison between CoCiP and APCEMM which establishes the degree of agreement in predictions of lifetime optical depth when six meteorological parameters are varied. The potential causes of the disagreements are investigated using arguments based on the physical understanding of contrail formation, persistence, and sublimation.

https://doi.org/10.5194/egusphere-2025-278
Preprint. Discussion started: 5 March 2025

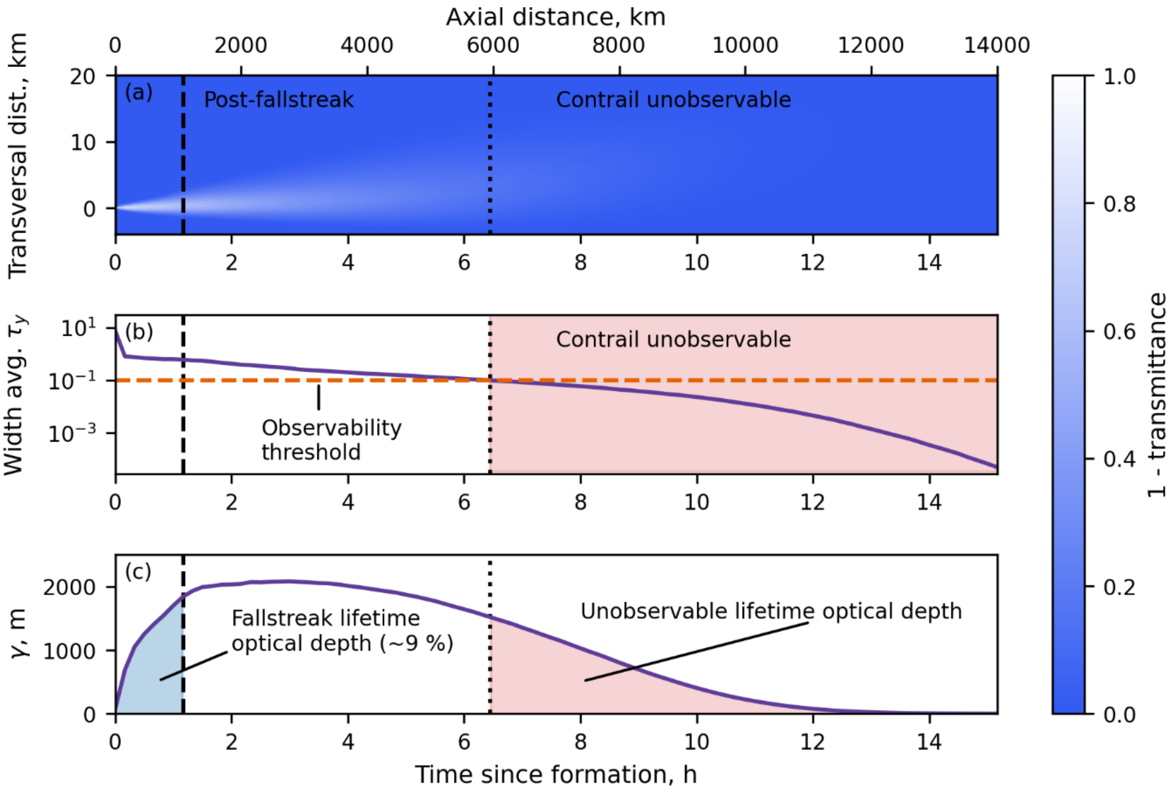

Figure 1: (a) Plan view contour plot of 1-transmittance (ratio of the light absorbed and reflected over the light received). (b) Width average vertical optical depth against time since formation. (c) Integrated optical depth against time since formation. The x axis can be interpreted as time (bottom) or as axial distance from the aircraft (top) if a constant aircraft speed is assumed. The vertical dashed line indicates the end of the fallstreak. The vertical dotted line indicates the time where the contrail crosses the observability threshold. This contrail was simulated in APCEMM using the default meteorology in this study (see Sect. 2.1).

1.1 Persistent contrails and contrail models

Contrails form in the aircraft plume when the Schmidt-Appleman criterion is satisfied (Schumann, 2012). For a contrail to persist, there must be ambient supersaturation with respect to ice. There are four regimes that a persistent contrail will experience throughout its lifetime: jet, vortex, dissipation, and diffusion (Gerz et al., 1998). Contrails which persist until the diffusion regime can spread up to ~40 km horizontally (Schumann et al., 2017) and hence have the potential to have a disproportionate climate impact. Teoh et al. (2024) shows that 10 % of flights which form persistent contrails (2 % of all flights) account for 80 % of the global annual energy forcing from contrails. For this reason, this investigation only considers the models in the diffusion regime.

https://doi.org/10.5194/egusphere-2025-278
Preprint. Discussion started: 5 March 2025

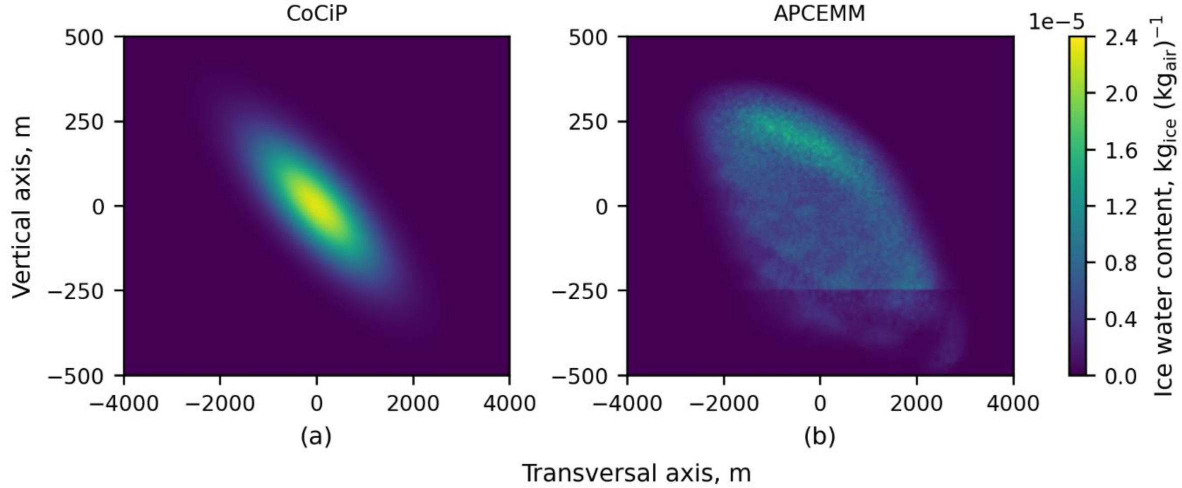

Figure 2: Cross-sectional distribution of the ice water content (IWC) for the CoCiP plume (a), and APCEMM plume (b) ~1h 30m after formation. Both simulations use the same meteorological conditions.

1.1.1 CoCiP

The Contrail Cirrus Prediction model (CoCiP) consists of a wake vortex sub-model, a Lagrangian Gaussian plume model, and a radiative balance model (Schumann, 2012). The CoCiP wake vortex sub-model initializes the Lagrangian Gaussian plume model in the diffusion regime, in which the concentration of water vapor and ice water is assumed to follow a Gaussian distribution in space (see Fig. 2(a)). The angle and standard deviations of the resulting ellipse are modified to simulate the effect of wind shear and diffusion, while the centroid of the ellipse descends to simulate the effect of ice crystal settling. The ambient conditions with which the plume interacts are treated as being uniform in space at each centroid position. For this reason, CoCiP can be referred to as a 0D model. For a given value of vertical wind shear, the area of the simulated cross section will increase until the contrail evaporates. Contrail evaporation in CoCiP occurs when the centroid ambient relative humidity with respect to ice falls below one or, in rare cases, when the contrail experiences excessive heating as it falls (see Appendix F). All ice crystal microphysics are represented through changes in two parameters: the total number of ice crystals and the total ice mass. The ice crystal size is a single value calculated from these quantities (Schumann, 2012). and is treated as being uniform across the contrail (i.e. the size distribution is monodisperse at any given time).

The CoCiP version used is from the pycontrails python library, an open-source project developed and maintained by members of Breakthrough Energy and Imperial College London (details in Appendix A).

1.1.2 APCEMM

The Aircraft Plume Chemistry, Emissions, and Microphysics Model (APCEMM) is “a Lagrangian model that explicitly models the chemical and microphysical evolution of an aircraft plume” (Fritz et al., 2020). APCEMM begins the contrail

https://doi.org/10.5194/egusphere-2025-278
Preprint. Discussion started: 5 March 2025

simulation with a box model for its vortex regime and then uses a 2D rectilinear grid to represent the contrail cross-section in the diffusion regime. This allows the APCEMM plume to take any shape (Fig. 2(b)). The transport and microphysical processes are computed at each grid cell. However, this grid is dynamic, meaning that the number of grid cells and the grid size change as the contrail expands. APCEMM uses a 38-bin sectional representation to approximate the ice particle size distribution in each grid cell.

APCEMM also represents ice particle loss mechanisms at a grid-cell level rather than at a contrail level (Fritz et al., 2020). Mesoscale turbulent temperature fluctuations were not present in the original version of APCEMM but are now simulated using random temperature fluctuations. At each timestep, APCEMM disturbs the temperature at each grid cell by a random value distributed within the range [-1, 1] K. This emulates the method used in Lewellen et al. (2014) to maintain ambient turbulence. The perturbation amplitude is left at 1 K throughout this investigation, and an initial seed of 0 has been chosen for all simulations to ensure reproducibility of the results.

2 Experimental design

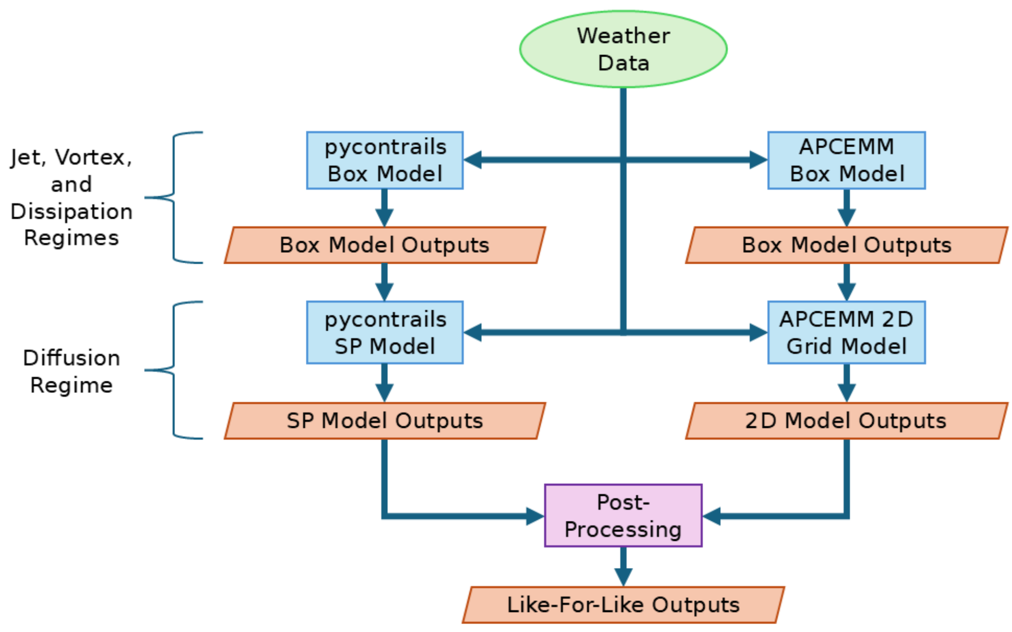

Figure 3: Flow chart showing the experimental simulation process for both CoCiP and APCEMM. Green ellipses indicate inputs, blue rectangles indicate plume models, orange rhombi indicate outputs, and purple rectangles indicate data processing units.

Figure 3 provides a flow chart overviewing the experimental process in this investigation. First, the model parameters are harmonized prior to the simulations (see Appendix C). Equivalent meteorological scenarios are then produced for each

https://doi.org/10.5194/egusphere-2025-278
Preprint. Discussion started: 5 March 2025

model, with each scenario described by six independent meteorological parameters (Section 2.1). We first compare results for a single representative scenario (Section 3), focusing on integral quantities such as total ice mass, average optical depth, and lifetime integrated optical depth. We then quantify the sensitivity of these integral quantities to different values of six different meteorological variables (Section 4).

2.1 Weather parametrization

All simulations use an idealized vertical weather profile consisting of a stable trapezoidal moist layer (Fig. 4), fully described by six independent meteorological variables. Ranges and default values for the six parameters are given in Table 1.

The layer RHi range was chosen to be above 100 % to ensure persistent contrail formation, with the highest layer RHi set to 140 % to remain beneath the homogeneous crystallization threshold of ~145 % RHi (Unterstrasser and Gierens, 2010a). The simulated range of supersaturated layer depths is chosen based on radiosonde data from the UK which showed that 53% of ice supersaturated regions are between 100 and 1500 m (Dickson et al., 2009). The transition between the super- and subsaturated regions is modelled with a constant gradient in RHi. The range of temperatures at cruise altitude is chosen based on estimates of typical values for northern hemisphere ice supersaturated regions (Spichtinger et al., 2003). We assume a uniform lapse rate of -6.5 K / km based on the International Standard Atmosphere. Finally, wind shear values are chosen to be consistent with the bounding scenarios of Unterstrasser and Görsch (2014). Each weather parameter is varied individually, with simulations performed at three parameter values. Contrails are not allowed to persist past 24 h.

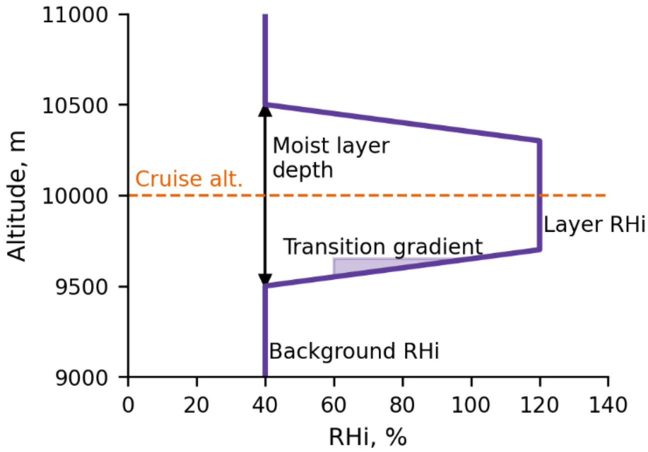

Figure 4: An example of a parametrized weather profile used in this investigation.

https://doi.org/10.5194/egusphere-2025-278
Preprint. Discussion started: 5 March 2025

Table 1: Values of the weather parameters used in this investigation. Only one parameter is varied at a time. Parameters not being varied take their baseline value, marked by an asterisk. The transition gradient at the default meteorology is infinite, making the moist layer rectangular in RHi.

Parameter	*Units*	*Low Value*	*Medium Value*	*High Value*
Background RHi	%	20	40*	60
Layer RHi	%	110	125*	140
Moist Layer Depth	m	500	1000*	1500
*Transition Gradient**	% m^{-1}	0.2	0.4	0.6
Temperature	K	208.15	215.65	223.15*
Wind Shear	s^{-1}	0.002*	0.004	0.006

2.2 Output processing and metrics

We use lifetime optical depth Γ as a proxy for climate impact. It is calculated as the integral over time and contrail width of the local optical depth in meter-hours (m h), such that

$$\gamma(t) = \int \tau_y(x,t)dx \,, \tag{1}$$

$$\Gamma = \int \gamma(t)dt, \tag{2}$$

where τ_y is the total vertical optical depth at a particular width coordinate x of the contrail cross-section, and γ is the vertical optical depth integrated across the contrail. The lifetime optical depth accounts for persistence, spread, and optical properties, making it implicitly related to climate impact. The lifetime optical depth is also directly computable from both models without requiring any assumptions regarding optical properties, local cloud cover, time of day, or any of the other parameters which would need to be defined for a radiative forcing calculation.

To evaluate the effects of each weather parameter on the lifetime optical depth, we define the sensitivity Φ as

$$\Delta\hat{\Gamma} = \frac{\Gamma_n - \Gamma_1}{\Gamma_{mid}}, \tag{3}$$

$$\Phi = \frac{\Delta\hat{\Gamma}}{\lambda_3 - \lambda_1}, \tag{4}$$

where $\Delta\hat{\Gamma}$ is the change in lifetime optical depth throughout the sweep of a single parameter normalized by the lifetime optical depth (Γ_{mid}) computed at the central parameter value, and λ is the value of the varied weather parameter at each simulation.

https://doi.org/10.5194/egusphere-2025-278
Preprint. Discussion started: 5 March 2025

3 Comparison of CoCiP and APCEMM for the baseline case

We first simulate a baseline meteorological scenario in both CoCiP and APCEMM. Results are provided in Section 3.1, followed by discussion and analysis in Section 3.2.

3.1 Results

Figure 5(a) shows the simulated contrail evolution in both CoCiP and APCEMM. The lifetime optical depth of this contrail in APCEMM (15500 m h) is four times that simulated by CoCiP (4000 m h). Additional metrics are provided in Appendix D.

The two models show qualitatively different behavior over the course of the contrail's lifetime. The CoCiP simulation exhibits a single sub-regime which we refer to as the "fallstreak". This phase is defined by continuous downwards acceleration as the settling crystals encounter unperturbed air, grow (albeit sharing this growth across all crystals in the contrail), accelerate, and reach new unperturbed air, with an average fall rate of 130 m h^{-1} until the contrail abruptly sublimates upon reaching the subsaturated air after 4 hours. The total number of ice crystals in the contrail per unit depth N (Fig 5c) decreases steadily at a rate of 0.21 decades per hour throughout the entire simulation.

The APCEMM simulation shows similar fallstreak behavior initially (~0–1 h), but with a small crystal loss rate of 0.05 decades per hour. It also ends sooner, as the lowermost crystals take up water and accelerate faster than the contrail-wide acceleration in CoCiP. However, rather than sublimating entirely at the end of this period, the descent rate of the remaining contrail slows. This defines the beginning of a second, "settled" sub-regime (~1–10 h) characterized by loss of ice crystals at a rate of 0.19 decades per hour, like that shown in the CoCiP fallstreak. After 10 hours the contrail enters a third, "fading" sub-regime (~10–15 h) characterized by the loss rate increasing to 0.59 decades per hour, which ends with complete sublimation of the contrail. From the fallstreak to the settled sub-regime the average fall speed of the APCEMM center of mass fall decreases from 147 m h^{-1} to 23 m h^{-1}, while the fall rate during the fading sub-regime approaches 0 m h^{-1}.

These differences are also reflected in the evolution of total contrail ice mass per unit length (Fig. 5(d)). Ice mass in CoCiP grows exponentially, whereas ice mass increase in APCEMM is closer to linear. In both models the total ice mass approaches a maximum at the end of the fallstreak sub-regime.

Through integration of Fig. 5(b), the fallstreak and post-fallstreak sub-regimes contribute 9 % and 91 % respectively to the APCEMM lifetime optical depth, compared to 100 % and 0 % for CoCiP. In absolute terms, the fallstreak sub-regime contributes ~4000 m h and ~1400 m h to the CoCiP and APCEMM lifetime optical depth respectively.

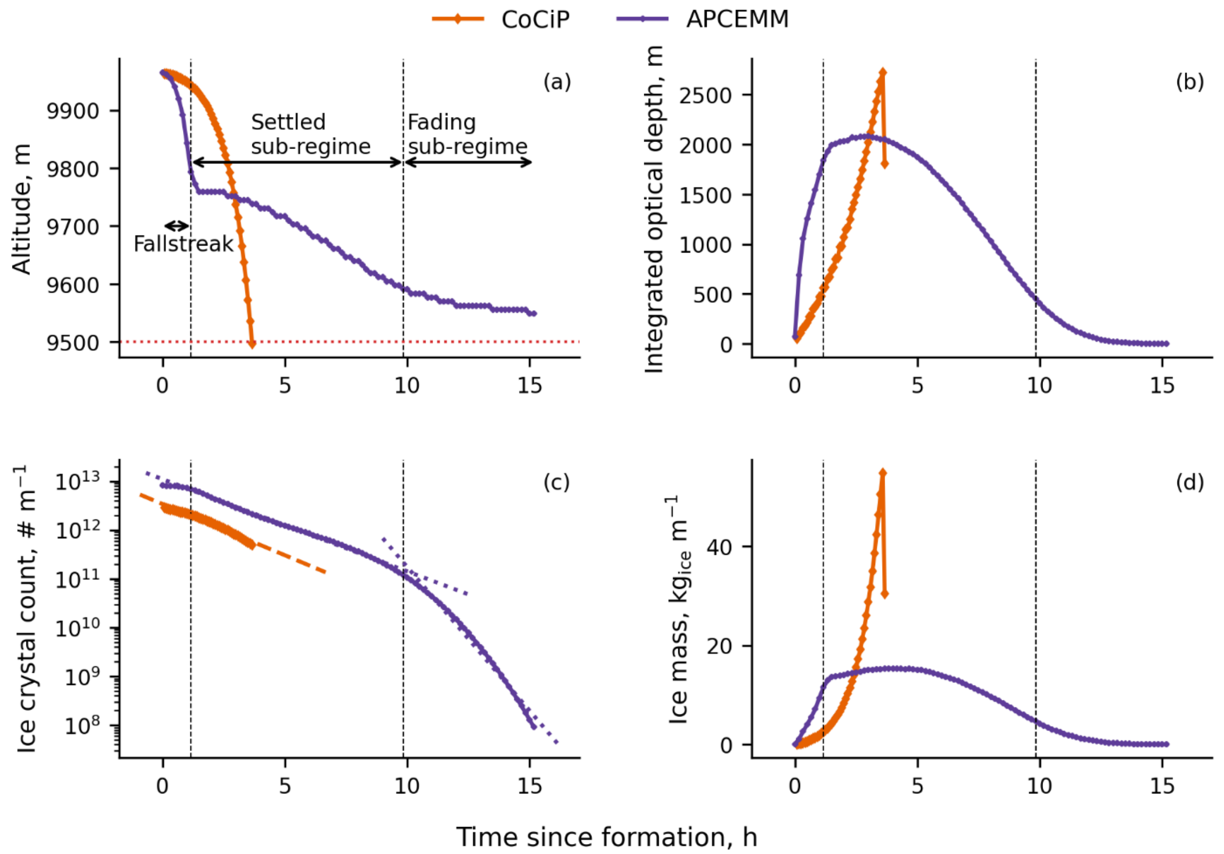

Figure 5: Evolution of contrail properties at the baseline meteorology. (a) Center of mass altitude against time. The dotted red horizontal line indicates the lower limit of the moist layer. (b) Integrated optical depth (γ) against time. (c) Total number of ice crystals (N) against time. The exponential decay fits for CoCiP and APCEMM are given by the dashed and dotted straight lines respectively. (d) Total ice mass (I) against time. The vertical lines mark the APCEMM sub-regime transition times.

3.2 Discussion

The differences in model behaviors observed in Fig. 5 can be explained by considering the contrail representations of each model. CoCiP defines its contrail properties at the center and uses a monodisperse ice crystal radius distribution, whereas APCEMM discretizes space into ~350 m^2 grid cells and uses 38 ice radius bins at each of these cells. This allows for ice crystals of different sizes to fall at different rates and separate spatially in APCEMM. Like in Lewellen (2014), the APCEMM contrail can be simplified into two components: "a core near flight level with larger number densities and a much more sparsely populated precipitation plume below with larger crystals" (Lewellen, 2014).

Using the simplified description of the contrail cross-section, mathematical definitions of the sub-regimes observed in Fig. 5 can be formulated by considering the total ice mass per unit length (I). First, the fallstreak is defined as the sub-regime in which the precipitation plume has not yet reached the subsaturated layer. Throughout the fallstreak $\frac{dI}{dt} > 0$ and $\frac{d^2I}{dt^2} > 0$ since

https://doi.org/10.5194/egusphere-2025-278
Preprint. Discussion started: 5 March 2025

water deposition outweighs sublimation. The settled sub-regime begins when the precipitation plume first reaches the subsaturated layer and the ice crystals begin to sublimate in it, characterized by $\frac{d^2I}{dt^2} \leq 0$. The fading sub-regime begins when the contrail core reaches the subsaturated layer. During the fading sub-regime $\frac{dI}{dt} < 0$ and $\frac{d^2I}{dt^2} > 0$ since the sublimation rate decreases progressively as fewer ice crystals remain. Since CoCiP cannot represent this differential sedimentation (see Sect. 4.2.2), which is typical of cirrus clouds (Sölch and Kärcher, 2010), it cannot represent the separation of the precipitation plume from the contrail core. CoCiP simulations therefore capture only fallstreak behavior (albeit with some anomalies due to certain model assumptions - see Appendix F). With this, the evolution of the remaining contrail properties in each sub-regime can now be considered.

During the fallstreak ice crystals grow rapidly in both models leading to the fastest center of mass fall rate (Fig. 5(a)). In CoCiP, the entire contrail moves with the center with the fall speed of the average ice particle. In APCEMM, the ice radius bins allow the large particles to fall the fastest, a form of gravitational size sorting which results in the formation of a precipitation plume beneath the contrail core. An enhancement to vertical diffusivity is applied to try and compensate for this in CoCiP (Schumann, 2012). Nonetheless, the CoCiP fallstreak descent rate is lower, the fallstreak sub-regime lasts longer, and the contrail acquires ice mass at a slower rate than in APCEMM.

When the large ice particles exit the supersaturated layer in the settled sub-regime they sublimate, making the contrail lose ice mass. In CoCiP this results in near-instantaneous evaporation, as the entire contrail experiences the same conditions. In APCEMM this instead results in a decrease in the center of mass fall rate from 147 m h^{-1} to 23 m h^{-1} (Fig. 5(a)) between the fallstreak and settled sub-regimes. Once the contrail core reaches the subsaturated region it enters the fading sub-regime, during which only the ice particles with the lowest fall rate remain. This results in a progressive decay in the center of mass fall speed and eventually contrail evaporation. A video of the contrail evolution simulated in APCEMM can be found in the Video Supplement.

Although many of the fundamental equations in CoCiP have been calibrated (Shapiro et al., 2024) to fit observations from the Contrails Library (COLI) database (Schumann et al., 2017), these adjustments cannot represent the transition of the contrail to a new sub-regime. Observations of long-lived contrails are also rare due to their low local optical depth. 25 % of the lifetime optical depth in APCEMM is produced at a point where the average optical depth is below 0.1, meaning that the aged APCEMM contrail would likely not be observable in from satellites (Kärcher et al., 2009). Properties and behaviour in the unobservable region are therefore particularly difficult to calibrate from observational data.

Post-fallstreak sub-regimes contribute ~91 % to the APCEMM lifetime optical depth but 0 % of the CoCiP lifetime optical depth (Fig. 5(b)). Post-fallstreak behavior has been observed in studies employing large eddy simulations (Unterstrasser and Gierens, 2010a, Lewellen et al. 2014, Lewellen, 2014). This does not imply the correctness of the APCEMM post-fallstreak behavior, but it does suggest that some post-fallstreak behavior should be expected for long-lived contrails.

https://doi.org/10.5194/egusphere-2025-278
Preprint. Discussion started: 5 March 2025

3.2.1 Implications for real contrails

The presence of post-fallstreak sub-regimes could have resulted from the controlled experimental setup relying on time-stable ISSRs, making it important to consider their typical lifetimes. Schumann (2012) analyzed ECMWF data for 6–9 June 2006 and found that 1 % of ISSRs had lifetimes over 24 h. Irvine et al. (2014) conducted a study tracking the advection of ISSRs in the North Atlantic using ECMWF Interim reanalysis data from three winter and summer seasons. Their results show that the mean lifetime (in a Lagrangian sense) for ISSRs is ~6 h, and that 5 % of ISSRs forming in the troposphere will have lifetimes exceeding 24 h, with their Fig. 4(a) indicating that the proportions of wintertime tropospheric ISSRs persisting for over 6, 12, 18, and 24 h are 32, 14, 6, and 2 % respectively. Overall, these studies indicate that time-stable ISSRs account for a non-negligible proportion of all ISSRs. This is further supported by a recent preprint (Hofer and Gierens, 2024) which analyzed a larger ECMWF dataset and found that contrail lifetime is most commonly limited by sedimentation, as opposed to advection of the contrail out of the ISSRs. This implies that, although the meteorology has been idealized in this study, the characterization of the sub-regimes observed in this study may have widespread applicability.

4 Effects of varying weather parameters

We now simulate 14 different meteorological scenarios, spanning variations in six different weather parameters (Table 1). We first compare the general trends in lifetime optical depth (Section 4.1.1) and then the sensitivity with respect to each parameter (Section 4.1.2).

4.1 Results

4.1.1 Lifetime optical depth

Figure 6(a) compares the lifetime optical depth from CoCiP and APCEMM when considering all contrail lifetime (orange) and when only considering the fallstreak (purple).

The CoCiP and APCEMM simulations disagree regardless of whether the entire lifetime is considered or the fallstreak is considered in isolation. When only the APCEMM fallstreak is considered, CoCiP simulations have lifetime optical depth values 3.2 times larger than those from the corresponding APCEMM fallstreak. The case in which all sub-regimes are considered lies above the parity line, with APCEMM simulations having a lifetime optical depth 3.8 times that of CoCiP.

The relationship between the proportion of lifetime optical depth in the fallstreak and unobservable regions is displayed in Fig. 6(b). Considering aggregate values, 92 % of all APCEMM lifetime optical depth is produced after the fallstreak sub-regime, and 35 % is produced when the contrail is unobservable. In contrast, CoCiP produces 0 % of its lifetime optical depth past the fallstreak, and 13 % past the observability threshold.

https://doi.org/10.5194/egusphere-2025-278
Preprint. Discussion started: 5 March 2025

4.1.2 Sensitivity to weather parameters

Despite the baseline differences the models mostly agree on the sign of the sensitivity of lifetime optical depth with regards to the six meteorological parameters (Table 2, Fig. 7). The exception is the sensitivity to moist layer RHi, where CoCiP finds a 1.2 % reduction in lifetime optical depth per percentage point increase in RHi compared to a 3.4 % increase in APCEMM. Although there is some anomalous behavior in CoCiP for the 110 % RHi case (see Figure 8 and Appendix F), the disagreement in sign remains even when this case is excluded.

Otherwise, both models show a decrease in Γ with increasing temperature and an increase in Γ with increases in all other parameters. The sign of the sensitivity is consistent whether considering the full APCEMM lifetime or only the fallstreak. The largest disagreement in the value of the sensitivity between APCEMM and CoCiP for the parameters where the sign agrees is in wind shear, (10 % per m/s/km for APCEMM, compared to 5.1 % in CoCiP). Figure 9 demonstrates this in terms of the effect of wind shear on altitude in each simulation, with settling velocities increasing with growing wind shear in CoCiP. In APCEMM, the settling velocity is unaffected during the fallstreak sub-regime but is similarly increased by increased wind shear during the post-fallstreak sub-regimes. Furthermore, at the end of the APCEMM fallstreak, the shear increases the contrail width by 143 % and the ice mass by 58 %, leading to a 36 % increase in lifetime optical depth between the 0.002 s^{-1} and the 0.006 s^{-1} shear cases (see Appendix D).

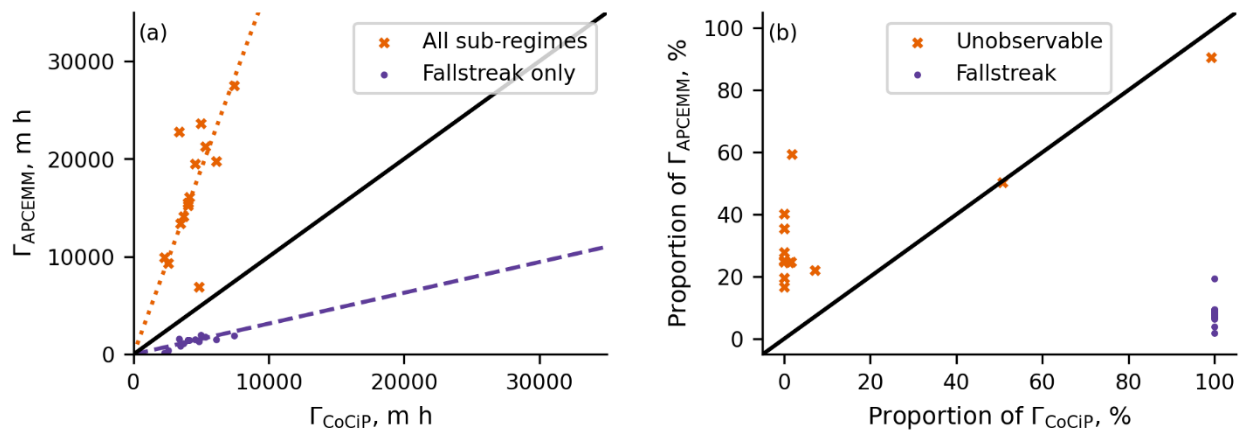

Figure 6: (a) Parity plot for the lifetime optical depth (Γ). The dotted line is the line of best fit for all sub-regimes, and the dashed line is the line of best fit for the fallstreak only. (b) Parity plot for the unobserbavle and fallstreak proportions of lifetime optical depth. The solid black line indicates the line of equality.

https://doi.org/10.5194/egusphere-2025-278
Preprint. Discussion started: 5 March 2025

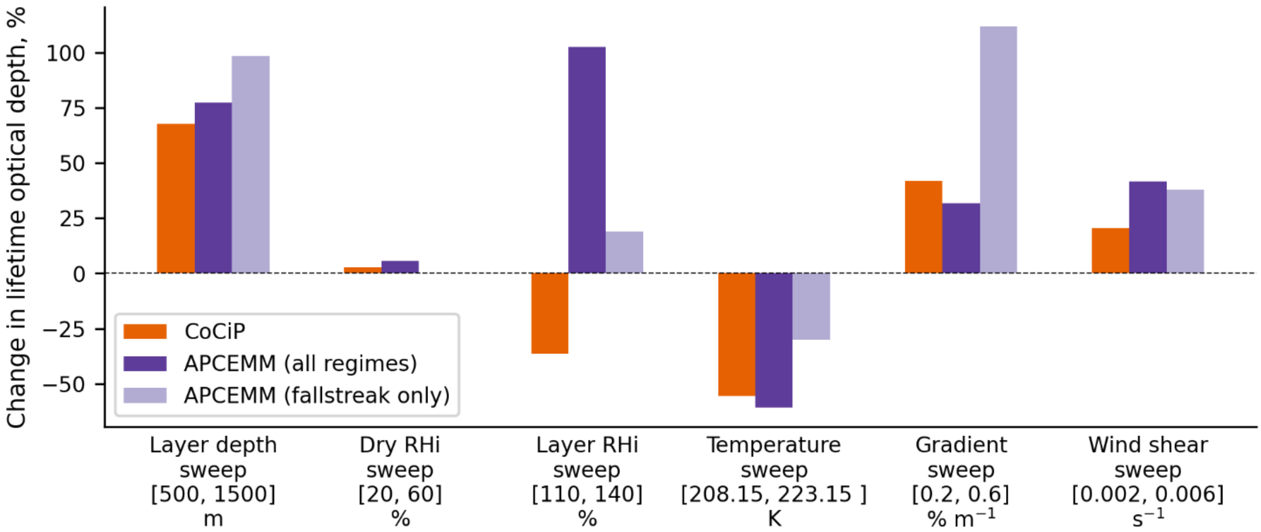

Figure 7: Bar chart showing the relative percentage change in lifetime optical depth across the contrail-producing simulations ($\Delta\hat{\Gamma}$) for each meteorological variable. A positive value indicates that an increase in a particular variable leads to an increase in the contrail lifetime optical depth.

Table 2: Sensitivity (Φ) of each weather parameter. A positive value of Φ indicates that increasing the parameter yields an increase in the lifetime optical depth (Γ). The APCEMM sensitivities to the temperature are underestimates because the contrail persists past the maximum simulation time of 24 h.

Parameter	*Φ units*	*APCEMM Φ*	*APCEMM fallstreak Φ*	*CoCiP Φ*
Background RHi	$\%_{change}(\Gamma)\cdot(\text{RHi }\%)^{-1}$	0.14	0.0024	0.070
Layer RHi	$\%_{change}(\Gamma)\cdot(\text{RHi }\%)^{-1}$	3.4	0.63	-1.2
Moist Layer Depth	$\%_{change}(\Gamma)\cdot\text{km}^{-1}$	77	99	68
Transition Gradient	$\%_{change}(\Gamma)\cdot(\text{RHi }\%\text{ km}^{-1})^{-1}$	0.080	0.28	0.10
*Temperature**	$\%_{change}(\Gamma)\cdot\text{K}^{-1}$	-4.0	-2.0	-3.7
Wind Shear	$\%_{change}(\Gamma)\cdot(\text{m s}^{-1}\text{ km}^{-1})^{-1}$	10	9.5	5.1

https://doi.org/10.5194/egusphere-2025-278
Preprint. Discussion started: 5 March 2025

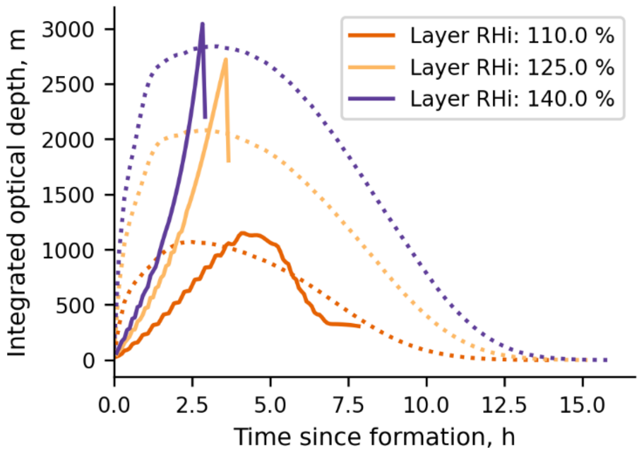

Figure 8: Integrated optical depth (γ) against time for the contrails produced at varying layer RHis. The CoCiP and APCEMM simulations are represented by solid and dotted lines respectively.

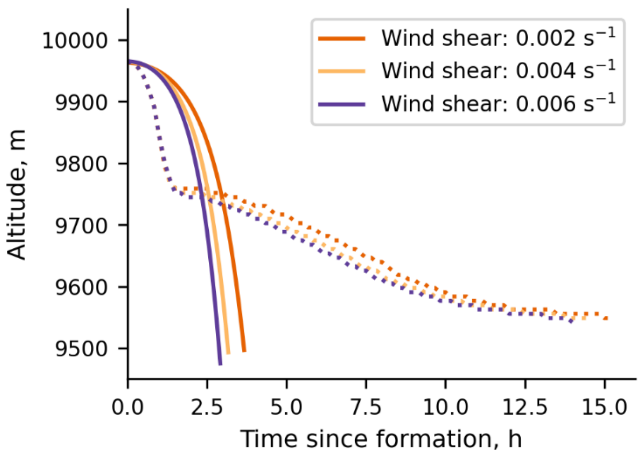

Figure 9: Center of mass altitude against time for the contrails produced at varying wind shear. The CoCiP and APCEMM simulations are represented by solid and dotted lines respectively.

4.2 Discussion

4.2.1 Extent of agreement in predicted lifetime optical depth

As in the baseline case (Section 3.1), APCEMM consistently predicts a shorter fallstreak sub-regime followed by longer post-fallstreak sub-regimes when compared to CoCiP. This explains why the CoCiP contrails last ~3 times longer than the corresponding APCEMM fallstreaks, with lifetime optical depths on average 3.2 times greater (Fig. 6(a)). This ratio reverses when the full contrail lifetime is considered however, and Fig. 6(b) shows that a higher proportion of integrated optical depth also occurs in APCEMM than in CoCiP after the contrail becomes “unobservable” (35 % and 13 % respectively). If post-

https://doi.org/10.5194/egusphere-2025-278
Preprint. Discussion started: 5 March 2025

fallstreak and post-observable behaviors are as important as suggested by APCEMM, approximations may be needed to extend 0D modelling techniques to the settled and fading sub-regimes.

Since almost all CoCiP contrails evaporate when the plume center reaches the subsaturated layer, the CoCiP contrails with large initial ice mass densities are much less likely to reach the observability threshold than the equivalent APCEMM contrails because they experience total evaporation more prematurely than the cases with low initial ice mass densities. This suggests that CoCiP might underestimate the climate impact of the contrails we already deem to be the most impactful. Nevertheless, further research is necessary to characterize the accuracy of the climate impact predictions from both CoCiP and APCEMM.

4.2.2 Extent of agreement in sensitivity

Varying the layer RHi causes the lifetime optical depth to decrease in CoCiP and increase in APCEMM. Fig. 1 in Lewellen (2014) shows that increasing the layer RHi increases the total ice crystal count, ice mass, and ice particle surface area throughout the contrail lifetime. Since the optical depth can be thought to increase with the contrail ice mass and ice surface area, it can be deduced that increasing the layer RHi would result in an increase in lifetime optical depth, and hence a positive sensitivity to the layer RHi. The CoCiP sensitivity to layer RHi is not consistent with APCEMM nor Lewellen (2014). This has implications for the implementation of robust contrail avoidance strategies, which require avoiding contrails with predicted characteristics agreed on by several models. Explaining disagreement in the sensitivity is hence necessary to be able to bridge the behaviors of the models.

The opposite sensitivity to the layer RHi occurs because most of the lifetime optical depth stems from the fallstreak for CoCiP and the post-fallstreak sub-regimes for APCEMM (see Sect. 3.2). For CoCiP, Fig. 8 shows that γ grows at higher rates as the layer RHi increases. This happens due to the associated increase in contrail ice mass. However, this effect competes with the decreasing lifetime caused by the increased settling speed of the larger ice particles in the higher layer RHi cases. Overall, the lifetime shortening effect outweighs the growth rate effect in Γ, leading to a negative sensitivity to the layer RHi in CoCiP (Table 2). For APCEMM, Fig. 8 shows that γ reaches larger values for higher layer RHis throughout the entire lifetime. Like in CoCiP, the fallstreak sub-regime in APCEMM terminates sooner with increasing layer RHi due to the increased rate of mass accumulation of the lowermost settling ice particles. However, the overall APCEMM lifetime increases. This makes the sensitivity for the APCEMM fallstreak (0.63 units, Table 2) ~6 times lower than the sensitivity of the entire APCEMM contrail (3.4 units, Table 2). The positive sensitivities confirm that the dominating effect for both the entire APCEMM lifetime and for the APCEMM fallstreak is the increase in γ with increasing layer RHi.

For the remaining variables, CoCiP and APCEMM both display similar sensitivity magnitudes, except for wind shear (Table 2, Fig. 7). Increasing the wind shear increases the contrail area horizontally and allows some crystals to settle into unperturbed air, hence leading to an increase in the amount of water uptake from the ambient air. The increased ice mass results in an increase in particle size, optical depth, and settling speed, although in theory this should not affect the lowermost particles which always fall through unperturbed air.

https://doi.org/10.5194/egusphere-2025-278
Preprint. Discussion started: 5 March 2025

The effect of the increased settling rate due to the increased particle size competes with the greater local optical depth and increased area. Lewellen (2014) find qualitatively similar results to APCEMM: increasing the shear leads to higher ice masses earlier and lower lifetimes. This leads to a limited increase in Γ with a moderate sensitivity to wind shear (5.1 units for CoCiP, 10 units for APCEMM, and 9.5 units for the APCEMM fallstreak, Table 2). APCEMM is approximately twice as sensitive to shear as CoCiP because, unlike APCEMM, CoCiP shows its increased settling rate throughout its lifetime due to the 0D nature of the model (Fig. 9). The APCEMM precipitation plume falls quickly and does not get exposed to much more unperturbed ambient air by the shear. This limits the water intake of the precipitation plume, limiting the increase in size of its ice particles. The lifetime of the APCEMM fallstreak hence appears unaffected (Fig. 9). Despite this, the shear in APCEMM does increase the contrail width at the end of the fallstreak by 143 % and the fallstreak ice mass by 58 %, leading to a 36 % increase in lifetime optical depth for the APCEMM fallstreak between the 0.002 s^{-1} and the 0.006 s^{-1} shear cases (see Appendix D). This shows that the slower moving core has time to take up more water than the precipitation plume, leading to the observation of an increased settling rate in the settled sub-regime with negligible increases to the settling rate during the fallstreak.

It is also helpful to consider the effect that wind shear has on a contrail once the fallstreak ends. For a real contrail in a constant shear environment, sublimation of the ice reaching the subsaturated layer causes the contrail shape to become truncated (see Fig. 2(b)). As the uppermost contrail crystals continue to settle and reduce the vertical extent of the contrail, this leads to a reduction in the contrail widening rate. In CoCiP the contrail instead continues to steadily gain ice through deposition as long as the centroid lies above the subsaturation point, and its cross-section continues to widen. Due to its spatially distributed ice particle size spectrum, the APCEMM contrail can show behavior closer to that expected from a real contrail.

4.2.3 Implications for contrail avoidance

Contrail avoidance which does not attempt to prioritize avoiding the most warming contrails can be performed without a contrail model, needing only an estimate of whether the Schmidt-Appleman criterion has been met. However, any further prioritization will necessarily be based on understanding the relationship between local meteorology, aircraft parameters, and the eventual contrail lifetime. Compared to simulations with APCEMM, contrails simulated in CoCiP have 3.8 times lower lifetime optical depths, the opposite sensitivity to changes in the local relative humidity, and approximately half the sensitivity to local wind shear. In the context of robust contrail avoidance strategies, the disagreement in baseline optical depth means that, due to the lack of post-fallstreak behavior, CoCiP predictions may underestimate the role of long-lived contrails including the potential for (typically cooling) daytime contrails to persist into nighttime and become warming. Meanwhile, the different sensitivities mean that the models will likely disagree regarding which contrails should be prioritized for avoidance.

https://doi.org/10.5194/egusphere-2025-278
Preprint. Discussion started: 5 March 2025

The two models do agree on the sign and order-of-magnitude of the relative sensitivity to other factors such as temperature and supersaturated layer depth. However, the results shown here suggest that efforts to prioritize specific contrails based on model-simulated radiative forcings may be premature.

5 Limitations and further work

We only consider a limited set of parameters in this work. We do not consider sensitivity to turbulence and vertical winds, which are parameters known to strongly affect contrail evolution. This means that the findings from this study cannot be generalized for all long-lived contrails. In addition, no evaluations have been performed with changes to more than one variable at a time. Furthermore, the inclusion of non-meteorological variables such as soot emissions, aircraft wingspan, and total mass would have provided further insights into the different processes captured by each model. Although sensitivity has been considered, the simulation conditions have been controlled and hence uncertainty has been neglected. Studies that extend the comparison to include model and weather uncertainty considerations are hence recommended.

6 Conclusions

The CoCiP and APCEMM contrail models fundamentally differ in terms of how they represent a contrail. CoCiP represents the contrail as a descending fallstreak, efficiently approximating the early behavior. However, APCEMM predicts two additional sub-regimes after the fallstreak, and our results suggest that these later sub-regimes provide 92% of the overall lifetime optical depth. This discrepancy in contrail representation means that the two models predict different magnitudes – and, for the local relative humidity, signs – of the relationships between the lifetime optical depth of a contrail and local meteorological parameters.

This work is highly idealized, considering only stable ice supersaturated regions which can support very long contrail lifetimes. However, tropospheric ice supersaturated regions are generally sufficiently large that the predominant mechanism for contrail evaporation is through sedimentation, as opposed to advection (Hofer and Gierens, 2024; Irvine et al., 2024). This makes the conceptual findings from this study applicable to real contrails, and hence to contrail avoidance. Nevertheless, the observed differences between the models are not just limited to the lack of post-fallstreak behavior in CoCiP.

This work suggests that strategies prioritizing the most warming contrails for avoidance (e.g. Teoh et al., 2024), although relevant for thought experiments, are likely not yet realizable in practice. Although physical arguments and prior large eddy simulation results provide some evidence that APCEMM is producing a more realistic simulation than CoCiP, this does not serve to validate or discredit either model. Further research and experiments are needed to characterize full lifetime contrail behaviour. This includes the challenging period where contrails are too thin to be easily observed from satellite, which we find to be responsible for 35% of total contrail lifetime optical depth in APCEMM simulations. Until efficient, reliable

https://doi.org/10.5194/egusphere-2025-278
Preprint. Discussion started: 5 March 2025

contrail models are available and backed by such evidence, our results suggest that contrail avoidance strategies which focus on avoidance of all contrails will have the greatest chance of producing a real climate benefit.

https://doi.org/10.5194/egusphere-2025-278
Preprint. Discussion started: 5 March 2025

Appendix A: CoCiP version and modifications

CoCiP simulations on the development version of pycontrails based on v0.54.0. The code branch used for this investigation was created from the 760244d commit (dated 16th Sept 2024) in the pycontrails main branch.

The following is a list of changes made to a fork of the pycontrails repo for this investigation. Model parameters that are not mentioned have been left at a default value:

- Increased the maximum contrail age from 20 to 24 h
- Decreased the integration timestep from 30 m to 5m to match APCEMM
- Removed the shear enhancement factor
- Force total and normal shear to take either of the following values depending on the case: 2e-3, 4e-3, or 6e-3 s^{-1}.
- Horizontal advection was disabled
- Forced the Brunt-Väisälä frequency to be 0.01 s^{-1} instead of being calculated from the meteorology
- Set the maximum contrail depth to infinity

See the Code Availability section for access to the code.

Appendix B: APCEMM version and modifications

APCEMM simulations on the development version based on v1.2.0. The branch of code used for this investigation was created from the c19b7f3 commit (dated 6th November 2024) in the APCEMM main branch. Modifications to APCEMM were made to enable the user selection of the random number generation seed.

See the Code Availability section for access to the code.

Appendix C: Aircraft and flight parameters

The aircraft used for this investigation was the Boeing 737-800. Table C1 shows the aircraft and flight parameters used in each model. Where no deterministic 1:1 relationship exists between equivalent parameters in each model, the closest default value was used.

Table C1: Aircraft and flight parameters used in this investigation. The values are estimates for a Boeing 737-800.

Flight Parameter Name	*Value*	*Units*	*In pycontrails?*	*In APCEMM?*	*Notes*
Cruise altitude	10000	m	✓	✓	264.36 hPa in APCEMM
Cruise speed	240	m s^{-1}	✓	✓	
Mach number	0.80	---	✓		Assumed constant
Brunt–Väisälä freq.	0.01	Hz	✓	✓	

https://doi.org/10.5194/egusphere-2025-278
Preprint. Discussion started: 5 March 2025

Soot EI	0.08	g kg^{-1}		✓	Equivalent to nvPM EI
Soot radius	$20 \cdot 10^{-9}$	m		✓	
nvPM EI	$1.19 \cdot 10^{15}$	# kg^{-1}	✓		
Total fuel flow	0.70	kg s^{-1}	✓	✓	
Number of engines	2	---	✓	✓	
Wingspan	34.32	m	✓	✓	
Wing area	124.6	m^2	✓		
Exit bypass area	0.9772	m^2		✓	
Engine efficiency	0.295	---	✓		No 1:1 equivalence with exit temp.
Core exit temperature	553.65	K		✓	No 1:1 equivalence with efficiency
Aircraft mass	60000	kg	✓	✓	
SO_2 EI	1.20	g kg^{-1}	✓	✓	
Latitude	52.1983	°	✓	✓	
Longitude	0.1202	°	✓	✓	

Appendix D: Tabulated lifetime optical depth results

Table D1: Lifetime optical depth for each model simulation that varies the background RHi.

Background RHi, %	*APCEMM Γ, m h*	*APCEMM fallstreak Γ, m h*	*CoCiP Γ, m h*
20	15224	1434	4032
40	15497	1434	4044
60	16112	1435	4146

Table D2: Lifetime optical depth for each model simulation that varies the layer RHi.

Layer RHi, %	*APCEMM Γ, m h*	*APCEMM fallstreak Γ, m h*	*CoCiP Γ, m h*
110	6890	1330	4854
125	15497	1434	4044
140	22794	1602	3382

Table D3: Lifetime optical depth for each model simulation that varies the moist layer depth.

Moist Layer Depth, m	*APCEMM Γ, m h*	*APCEMM fallstreak Γ, m h*	*CoCiP Γ, m h*
500	9302	372	2552
1000	15497	1434	4044
1500	21290	1785	5293

Table D4: Lifetime optical depth for each model simulation that varies the transition gradient. The mid-range parameter value is 0.6 % m^{-1}.

Transition Gradient, % m^{-1}	*APCEMM Γ, m h*	*APCEMM fallstreak Γ, m h*	*CoCiP Γ, m h*
0.2	9890	173	2263
0.4	13370	852	3455
0.6	14144	1126	3707
∞	15497	1434	4044

Table D5: Lifetime optical depth for each model simulation that varies the temperature.

Temperature, K	*APCEMM Γ, m h*	*APCEMM fallstreak Γ, m h*	*CoCiP Γ, m h*
208.15	27494	1892	7449
215.65	19748	1524	6114
223.15	15497	1434	4044

Table D6: Lifetime optical depth for each model simulation that varies the wind shear.

Wind Shear, s^{-1}	*APCEMM Γ, m h*	*APCEMM fallstreak Γ, m h*	*CoCiP Γ, m h*
0.002	15497	1434	4044
0.004	19489	1504	4549
0.006	23625	2003	4971

Appendix E: Prominence of CoCiP and APCEMM in academic works

Two metrics were used to determine the prominence of CoCiP and APCEMM: the citation number for the relevant model articles and the number of academic works either model has been mentioned in. Both metrics were extracted from Google Scholar.

Schumann (2012), the article which introduced CoCiP, has been cited 141 times, whereas Fritz et al (2020), the article which introduced APCEMM, has been cited 27 times as of the 25th of September 2024. CoCiP has approximately 5 times the citation count that APCEMM has.

The number of academic works that mention specific models is the number of results in a Google Scholar search with specific search terms, given below:

- Contrail models: *“contrail cirrus prediction model” OR APCEMM OR "contrail model" OR "contrails model" OR "contrails models" OR "contrails model"-myuouue*
- CoCiP: *“contrail cirrus prediction model”*
- APCEMM: *APCEMM -myuouue*

Note that the term -*myuouue* was used to remove a specific article that contained APCEMM but was unrelated to contrail modelling.

As of the 25th of September 2024, the number of mentions was as follows: 348 for contrail models, 185 for CoCiP, and 21 for APCEMM. CoCiP and APCEMM are hence mentioned in ~50% and ~5% of articles mentioning contrail models. Please note that these are only rough estimates.

Appendix F: Explanation of the anomalous CoCiP result at 110 % layer RHi

In Fig. 8, the CoCiP simulation at 110 % layer RHi shows a decrease in γ that does not correspond to post-fallstreak behavior. CoCiP has been formulated such that all the water content in the contrail (both vapor and ice) moves together with the contrail center. This water is isolated from the ambient humidity, except for the water added to the core to emulate mixing. If the ambient conditions are at or above ice saturation, the water mass in the CoCiP contrail is distributed between water vapor and ice to ensure that the air in the contrail is ice saturated. As the contrail falls, the ambient temperature increases due to the atmospheric lapse rate. The higher temperature leads to an increase in the amount of water required to maintain saturation with respect to ice. Initially, mixing with ambient air supplies more water than that required to maintain saturation, so the excess water is used to grow the ice crystals. Since the saturation humidity grows in a superlinear manner with temperature, as the contrail falls progressively larger amounts of water from mixing with the ambient air are required to maintain ice supersaturation. After 5 h the increase in water required to maintain saturation is no longer met by mixing. This causes the ice crystals to evaporate to maintain saturation with respect to ice, as dictated by the CoCiP formulation. This leads to a decrease in both the ice mass and γ and, eventually, to the contrail evaporation within the moist layer. This behavior is not accurate because the ice crystals fall independently of the water vapor in reality. Note that the 110 % layer RHi case has not been excluded from the results of this study because the effect is present in all the CoCiP simulations, despite it only being clearly visible in the 110 % layer RHi case (see Appendix F).

https://doi.org/10.5194/egusphere-2025-278
Preprint. Discussion started: 5 March 2025

Code availability

The code necessary to produce the simulations and results from this investigation is available at https://doi.org/10.5281/zenodo.14708885.

The modified pycontrails code is available at https://doi.org/10.5281/zenodo.14639631.

The modified APCEMM code is available at https://doi.org/10.5281/zenodo.14640899.

Video supplement

A set of videos showing the evolution of the APCEMM simulated contrail cross-section at the default meteorology is available at https://doi.org/10.5281/zenodo.14709364

Author contribution

CAM modified the CoCiP code, wrote the post-processing code and performed the simulations. SE helped with the HPC setup and provided technical guidance. JPJ set the overall scope of the manuscript, and the structure of the experimental design. CAM prepared the manuscript with reviews and edits from all co-authors.

Competing interests

The authors declare that they have no conflict of interest.

Acknowledgements

The authors would like to thank Dr. Jessie R. Smith for reviewing early versions of this work. The authors would also like to thank Paul Bond for his help setting up APCEMM initially, and for Michael Xu for the help with the APCEMM troubleshooting. The authors would also like to thank Tristan Abbott for his assistance in understanding the cause of the outlier CoCiP behavior associated with 125 % layer RHi. This work was supported by the UK Engineering and Physical Sciences Research Council [grant number EP/W524633/1]. For the purpose of open access, the authors have applied a Creative Commons Attribution (CC BY) license to any Author Accepted Manuscript version arising. This work was performed using resources provided by the Cambridge Service for Data Driven Discovery (CSD3) operated by the University of Cambridge Research Computing Service (www.csd3.cam.ac.uk), provided by Dell EMC and Intel using Tier-2 funding from the Engineering and Physical Sciences Research Council (capital grant EP/T022159/1), and DiRAC funding from the Science and Technology Facilities Council (www.dirac.ac.uk).

https://doi.org/10.5194/egusphere-2025-278
Preprint. Discussion started: 5 March 2025

References

Akhtar Martinez, C. and Jarrett, J. P.: Comparing Two Contrail Models Under Certain and Uncertain Inputs, in: AIAA SciTech 2024 Forum, Orlando, Florida, USA, 8-12 January 2024, AIAA 2024–1023, https://doi.org/10.2514/6.2024-1023, 2024.

Dickson, N., Gierens, K., Rogers, H., and Jones, R.: Vertical spatial scales of ice supersaturation and probability of ice supersaturated layers in low resolution profiles of relative humidity, in: Proceedings of the 2nd International Conference on Transport, Atmosphere and Climate, Aachen, Germany, and Maastricht, Netherlands, 22–25 June 2009, 239–247, 2009.

Fritz, T. M., Eastham, S. D., Speth, R. L., and Barrett, S. R. H.: The role of plume-scale processes in long-term impacts of aircraft emissions, Atmos. Chem. Phys., 20, 5697–5727, https://doi.org/10.5194/acp-20-5697-2020, 2020.

Gerz, T., Dürbeck, T., and Konopka, P.: Transport and effective diffusion of aircraft emissions, J. Geophys. Res.-Atmos., 103, 25 905–25 913, https://doi.org/10.1029/98JD02282, 1998.

Hofer, S. M. and Gierens, K. M.: Kinematic properties of regions that can involve persistent contrails, EGUsphere [preprint], 2024, 1–23, https://doi.org/10.5194/egusphere-2024-3520, 2024.

Irvine, E. A., Hoskins, B. J., and Shine, K. P.: A Lagrangian analysis of ice-supersaturated air over the North Atlantic, J. Geophys. Res.-Atmos., 119, 90–100, https://doi.org/10.1002/2013JD020251, 2014.

Kärcher, B., Burkhardt, U., Unterstrasser, S., and Minnis, P.: Factors controlling contrail cirrus optical depth, , Atmos. Chem. Phys., 9, 6229–6254, https://doi.org/10.5194/acp-9-6229-2009, 2009.

Lee, D., Fahey, D., Skowron, A., Allen, M., Burkhardt, U., Chen, Q., Doherty, S., Freeman, S., Forster, P., Fuglestvedt, J., Gettelman, A., De León, R., Lim, L., Lund, M., Millar, R., Owen, B., Penner, J., Pitari, G., Prather, M., Sausen, R., and Wilcox, L.: The contribution of global aviation to anthropogenic climate forcing for 2000 to 2018, Atmos. Environ., 244, 117834, https://doi.org/10.1016/j.atmosenv.2020.117834, 2021.

Lewellen, D. C., Meza, O., and Huebsch, W.: Persistent Contrails and Contrail Cirrus. Part I: Large-Eddy Simulations from Inception to Demise, J. Atmos. Sci., 71, 4399–4419, https://doi.org/10.1175/JAS-D-13-0316.1, 2014.

https://doi.org/10.5194/egusphere-2025-278
Preprint. Discussion started: 5 March 2025

Lewellen, D. C.: Persistent Contrails and Contrail Cirrus. Part II: Full Lifetime Behavior, J. Atmos. Sci., 71, 4420 – 4438, https://doi.org/10.1175/JAS-D-13-0317.1, 2014

Schumann, U.: A contrail cirrus prediction model, Geosci. Model Dev., 5, 543–580, https://doi.org/10.5194/gmd-5-543-2012, 2012.

Schumann, U., Baumann, R., Baumgardner, D., Bedka, S. T., Duda, D. P., Freudenthaler, V., Gayet, J.-F., Heymsfield, A. J., Minnis, P., Quante, M., Raschke, E., Schlager, H., Vázquez-Navarro, M., Voigt, C., and Wang, Z.: Properties of individual contrails: a compilation of observations and some comparisons, Atmos. Chem. Phys., 17, 403–438, https://doi.org/10.5194/acp-17-403-2017, 2017.

Shapiro, M., Engberg, Z., Teoh, R., Stettler, M., Dean, T., and Abbott, T.: pycontrails: Python library for modeling aviation climate impacts, https://doi.org/10.5281/zenodo.13770281, 2024.

Spichtinger, P., Gierens, K., and Read, W.: The global distribution of ice-supersaturated regions as seen by the Microwave Limb Sounder, Q. J. Roy. Meteor. Soc., 129, 3391–3410, https://doi.org/10.1256/qj.02.141, 2003.

Sölch, I. and Kärcher, B.: A large-eddy model for cirrus clouds with explicit aerosol and ice microphysics and Lagrangian ice particle tracking, Q. J. Roy. Meteor. Soc., 136, 2074–2093, https://doi.org/10.1002/qj.689, 2010.

Teoh, R., Schumann, U., Majumdar, A., and Stettler, M. E. J.: Mitigating the Climate Forcing of Aircraft Contrails by Small-Scale Diversions and Technology Adoption, Environ. Sci. Technol., 54, 2941–2950, https://doi.org/10.1021/acs.est.9b05608, 2020a.

Teoh, R., Schumann, U., and Stettler, M. E. J.: Beyond Contrail Avoidance: Efficacy of Flight Altitude Changes to Minimise Contrail Climate Forcing, Aerospace, 7, 121, https://doi.org/10.3390/aerospace7090121, 2020b.

Teoh, R., Engberg, Z., Schumann, U., Voigt, C., Shapiro, M., Rohs, S., and Stettler, M. E. J.: Global aviation contrail climate effects from 2019 to 2021, Atmos. Chem. Phys., 24, 6071–6093, https://doi.org/10.5194/acp-24-6071-2024, 2024.

Unterstrasser, S. and Gierens, K.: Numerical simulations of contrail-to-cirrus transition – Part 1: An extensive parametric study, Atmos. Chem. Phys., 10, 2017–2036, https://doi.org/10.5194/acp-10-2017-2010, 2010a.

https://doi.org/10.5194/egusphere-2025-278
Preprint. Discussion started: 5 March 2025

Unterstrasser, S. and Gierens, K.: Numerical simulations of contrail-to-cirrus transition – Part 2: Impact of initial ice crystal number, radiation, stratification, secondary nucleation and layer depth, Atmos. Chem. Phys., 10, 2037–2051, https://doi.org/10.5194/acp-10-2037-2010, 2010b.

Unterstrasser, S. and Görsch, N.: Aircraft-type dependency of contrail evolution, J. Geophys. Res.-Atmos., 119, 14015–14027, https://doi.org/10.1002/2014JD022642, 2014.

Xu, M.: Development and Evaluation of Contrail Models, M.S. Thesis, Massachusetts Institute of Technology, https://hdl.handle.net/1721.1/155484, 2024.

Wolf, K., Bellouin, N., and Boucher, O.: Sensitivity of cirrus and contrail radiative effect on cloud microphysical and environmental parameters, Atmos. Chem. Phys., 23, 14 003–14 037, https://doi.org/10.5194/acp-23-14003-2023, 2023.